Simplified Model to Study the Induction Generator Effect of the Sub-Synchronous Resonance Phenomenon

F. Bizzarri, *Senior Member, IEEE*, A. Brambilla *Member, IEEE*, F. Milano, *Fellow, IEEE*

***Abstract*— This letter presents a simple model of induction machines able to appraise the induction generator effect of the sub-synchronous resonance phenomenon. The proposed model is general and can be applied to induction machines utilized in wind power applications, such as doubly-fed induction generators. A rigorous stability analysis is carried out based on the proposed model. This analysis shows that the induction generator effect leads to a Neimark-Sacker bifurcation.**

***Index Terms*— Sub-synchronous resonance, induction generator effect, Neimark-Sacker bifurcation, doubly-fed induction generator.**

I. Introduction

The sub-synchronous resonance (SSR) effect has been largely studied since the first evidence in 1971 when generators of a steam power plant were damaged (and also before this event, see for example [1]–[5]). Literature classifies the SSR as induction generator effect (IGE), torsional interaction (TI) and torsional amplification (TA) [1]. The onset of SSR is explained by observing that the synchronous generator embeds a "parasitic" induction generator. If the stator "sees" a rotor turning at a frequency above the synchronous one, then the slip is negative and the equivalent circuit exhibits a negative resistance [5].

In the past, IGE was mostly considered an academic problem since, although possible, it was never seen in practice for synchronous generators. This situation, however, has considerably changed in the last decade due to the increasing penetration of wind power plants based on doubly-fed induction machines. Recent works show that SSR can occur for compensated wind power plants [6] and that the IGE is actually a significant issue in real-world applications [7], [8].

Existing literature on IGE is based on a parametric eigenvalue analysis. Typical studies show that the onset of the SSR phenomenon originates from an Hopf bifurcation (HB), which leads to the appearance of a limit cycle. This letter tackles the IGE from a circuital point of view and carries out a thorough bifurcation analysis to study the stability of the aforementioned limit cycle. The letter shows that, depending on the amount of capacitive compensation, the limit cycle can undergo a Neimark-Sacker bifurcation (NSB), thus becoming unstable and generating a torus. Whenever the newborn torus is unstable, The occurrence of the NSB makes the SSR phenomenon critical as it can lead to unbounded oscillations and collapse. The letter also suggests simple remedial actions to reduce the risk of or prevent at all the occurrence of the IGE.

II. Modelling

A symmetrical three-phase AC system can be represented through a two-phase equivalent in the $\alpha\beta$-frame through the well-known Clarke transform. Let's consider an induction machine with a capacitor connected in series to the stator impedance. In the $\alpha\beta$-frame and per unit, such a system can be described by the following set of equations [9]:

$$\begin{aligned}
&\phi_{\alpha s}(t) = L_s \imath_{\alpha s}(t) + \cos(\delta_r(t)) M \imath_{\alpha r}(t) - \sin(\delta_r(t)) M \imath_{\beta r}(t)\\
&\phi_{\beta s}(t) = L_s \imath_{\beta s}(t) + \sin(\delta_r(t)) M \imath_{\alpha r}(t) + \cos(\delta_r(t)) M \imath_{\beta r}(t)\\
&\phi_{\alpha r}(t) = \cos(\delta_r(t)) M \imath_{\alpha s}(t) + \sin(\delta_r(t)) M \imath_{\beta s}(t) + L_r \imath_{\alpha r}(t)\\
&\phi_{\beta r}(t) = \cos(\delta_r(t)) M \imath_{\beta s}(t) - \sin(\delta_r(t)) M \imath_{\alpha s}(t) + L_r \imath_{\beta r}(t)\\
&\dot{\phi}_{\alpha s}(t) + R_s \imath_{\alpha s}(t) - v_{\alpha s}(t) - E_{\alpha s} = 0\\
&\dot{\phi}_{\beta s}(t) + R_s \imath_{\beta s}(t) - v_{\beta s}(t) - E_{\beta s} = 0\\
&\dot{\phi}_{\alpha r}(t) + R_r \imath_{\alpha r}(t) - E_{\alpha r} = 0\\
&\dot{\phi}_{\beta r}(t) + R_r \imath_{\beta r}(t) - E_{\beta r} = 0\\
&C_s \dot{v}_{\alpha s}(t) + \imath_{\alpha s}(t) = 0\\
&C_s \dot{v}_{\beta s}(t) + \imath_{\beta s}(t) = 0\\
&\tau_e(t) = \phi_{\alpha s}(t) \imath_{\beta s}(t) - \phi_{\beta s}(t) \imath_{\alpha s}(t)\\
&\dot{\delta}_r(t) - \Omega \omega_r(t) = 0\\
&2H \dot{\omega}_r(t) - \tau_m + \tau_e(t) + D \omega_r(t) = 0\ ,
\end{aligned} \tag{1}$$

where s and r suffixes refer to quantities related to the stator and rotor, respectively; the upper dot symbol means time derivative; Ω is the nominal frequency in $\mathrm{rad\,s^{-1}}$; ϕ, $\imath$ and v indicate magnetic fluxes, currents and voltages, respectively; E are imposed voltages; L_s is the sum of the self-inductances of the stator coils and of the equivalent line; L_r is the self-inductances of the rotor coils; $M = k\sqrt{L_s L_r}$ is the peak value of the mutual inductance that periodically varies according to the mutual positions of the turns; $k \in (-1, 1)$ is the coupling coefficient; ω_s and ω_r are the angular speed with which stator and rotor coils rotate around their common rotational, respectively; R_r models the resistance of the rotor coils whereas R_s models the overall resistance of both the stator coils and the line; C_s models line capacitive compensation, i.e., it is assumed that the overall reactance of the line at the SSR frequency is capacitive; and H, D and τ_m are the inertia, the damping coefficient and torque of the single-mass generator, respectively.

The TI and TA phenomena are due to the interaction of the last two equations of (1) with the electrical system. The IGE, instead, originates exclusively from the coupling of electrical and magnetic equations of the machine and the compensated line. Since this letter focuses on the IGE only, the last three equations in (1) are dropped and thus $\delta_r(t)$ is imposed. This allows reducing the dynamic order of the system.

Since our goal is to define the minimal set of equations that shows the IGE, let us proceed as follows. First we define complex vectors of the $\alpha\beta$ components of fluxes, currents and voltages. So, for example, considering the stator current:

$$\bar{\imath}_s(t) = \imath_{\alpha s}(t) + j \imath_{\beta s}(t)\ . \tag{2}$$

Using this notation, electrical and magnetic equations of (1) can be

Federico Bizzarri and Angelo Brambilla are with DEIB, Politecnico di Milano, p.za Leonardo da Vinci 32, I20133 Milano, Italy. E-mail: {federico.bizzarri, angelo.brambilla}@polimi.it

Federico Bizzarri is also with the Advanced Research Center on Electronic Systems "E. De Castro" (ARCES), University of Bologna, Italy.

Federico Milano is with the School of Electrical and Electronic Engineering, University College Dublin, Belfield, Ireland. E-mail: federico.milano@ucd.ie

rewritten as:

$$\begin{aligned}
&\bar{\phi}_s(t) = L_s\bar{\imath}_s(t) + \exp(j\delta_r(t))M\bar{\imath}_r(t)\\
&\bar{\phi}_r(t) = \exp(-j\delta_r(t))M\bar{\imath}_s(t) + L_r\bar{\imath}_r(t)\\
&\dot{\bar{\phi}}_s(t) + R_s\bar{\imath}_s(t) - \bar{v}_s(t) - \bar{E}_s = 0\\
&\dot{\bar{\phi}}_r(t) + R_r\bar{\imath}_r(t) - \bar{E}_r = 0\\
&C_s\dot{\bar{v}}_s(t) + \bar{\imath}_s(t) = 0\ .
\end{aligned} \tag{3}$$

This set of equations is formally equivalent to a *single-phase* machine with *complex* time-varying fluxes, currents and voltages. This equivalency does not apply to the expression of the electromagnetic torque. However, since we are not interested in the mechanical equations of the machines, the formal equivalence holds.

To carry out the bifurcation analysis, we consider the single-mass two-coil system shown in Fig. 1, which is the real-domain version of (3). The resulting set of equations is:

$$\begin{aligned}
&\phi_s(t) = L_s\imath_s(t) + \sin(\delta_r(t))M\imath_r(t)\\
&\phi_r(t) = \sin(-\delta_r(t))M\imath_s(t) + L_r\imath_r(t)\\
&\dot{\phi}_s(t) + R_s\imath_s(t) - v_s(t) - E_s = 0\\
&\dot{\phi}_r(t) + R_r\imath_r(t) - E_r = 0\\
&C_s\dot{v}_s(t) + \imath_s(t) = 0\ .
\end{aligned} \tag{4}$$

This is the minimal set of equations that allows studying the IGE. The rationale for utilizing a simplified model is that the derivation of an accurate and reliable set of differential-algebraic equations describing the three-phase dynamic system does not add information on the SSR phenomenon [2], [3].

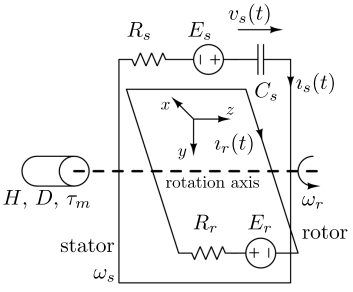

Fig. 1. The schematic of a distributed-lumped simplified equivalent circuit used to describe the onset of the IGE.

In normal operation, (4) exhibits a stable equilibrium. If this equilibrium undergoes a HB, then the limit cycle originated by the HB leads to the SSR. The evolution of the limit cycle can be studied as a function of the line parameters.

The $\delta_r(t)$ time varying angle modulates the $\sin(\,\cdot\,)$ functions in the flux equations, therefore any variation of ω_r reflects in the slip between the rotor and stator time-varying fluxes. Let us define a slip variable $\sigma = \omega_r - \omega_s$ and study a "specific" limit cycle originated at the HB point, i.e., a limit cycle whose period is $2\pi/\sigma$.

With simple algebraic transformations, (4) can be rewritten as:

$$\begin{aligned}
&\overbrace{\begin{bmatrix} L_s & -M\sin(\sigma t) & 0\\ M\sin(\sigma t) & L_r & 0\\ 0 & 0 & C_s \end{bmatrix}}^{\mathbf{A}(t)} \begin{bmatrix} \imath_s(t)\\ \imath_r(t)\\ \dot{v}_s(t)\end{bmatrix} =\\
&\underbrace{\begin{bmatrix} -R_s & M\sigma\cos(\sigma t) & 1\\ -M\sigma\cos(\sigma t) & -R_r & 0\\ -1 & 0 & 0 \end{bmatrix}}_{\mathbf{B}(t)} \begin{bmatrix} \imath_s(t)\\ \imath_r(t)\\ v_s(t)\end{bmatrix} + \begin{bmatrix} E_s\\ E_r\\ 0\end{bmatrix}
\end{aligned} \tag{5}$$

If $\sigma = 0$, the first and second equations in (5) are decoupled, $\mathbf{A}(t)$ and $\mathbf{B}(t)$ are constant, and the system admits a stable equilibrium point. This means that, for $\sigma = 0$, the IGE cannot occur. This is the typical operation condition of synchronous machines. For these machines, the condition $\sigma \neq 0$ occurs only during transients triggered by large disturbances. This is the reason why the IGE is unlikely for conventional power plants. However, for constant speed and/or doubly-fed induction generators, as those utilized in wind farms, $\sigma \neq 0$ always applies during normal operation. This makes the IGE a relevant phenomenon, as shown in the case study below.

The detailed model (1) and proposed model (4) behave in the same way until the occurrence of the NSB. This is so because, before the NSB, the effect of the mechanical equations and controllers (if considering a DFIG configuration), do not affect the coupling of machine electrical and magnetic equations. After the NSB, the mechanical equations do play an important role in the machine dynamics, i.e., the rotor speed decreases and the currents increase. Also the coupling between the α and β axis is not immaterial after the NSB. However, (4) is enough to define "where" the bifurcation occurs and provides information on how to keep the operating point of the machine away from such a bifurcation. This is illustrated through a numerical example in the following section.

III. Case Study

Let assume that σ is constant and equal to zero in (5) and check whether, for some values of the model parameters, the parasitic induction machine leads to an unstable and unbounded – i.e., catastrophic – dynamical evolution.

Figure 2 shows the results of a stability analysis that assumes C_s and R_s as bifurcation parameters. We focus first on the black continuous curve in Fig. 2, which represents the locus of NSBs [10]. To explain the changes in the dynamic response of the system, let us consider the dashed vertical line for $R_s = 0.02$ p.u. At P_1, the system admits a stable periodic steady state solution and the corresponding limit cycle, say Γ, undergoes a NSB at NS_1 by increasing C_s. As a consequence, the stability of Γ is lost and the system either admits a quasi-periodic behavior or, as it happens in this case study, becomes asymptotically unstable. The whole light yellow region inside the continuous black curve is unstable and characterized by unbounded oscillations. By further increasing C_s, Γ undergoes a further Neimark-Sacker bifurcation at NS_2 and, after that, becomes stable again (e.g., P_3).

The sequence of bifurcations illustrated above is slightly modified by increasing L_s, which leads to the gray curve in Fig. 2. This curve also represents the locus of NSBs. For illustration, Fig. 3 shows the trajectories projected on the $(\imath_s, \imath_r)$ plane obtained for the parameters values corresponding to P_2 in Fig. 2. In particular, the gray line represents a portion of the unbounded solution whereas the black line corresponds to the Γ limit cycle that is unstable in P_2.

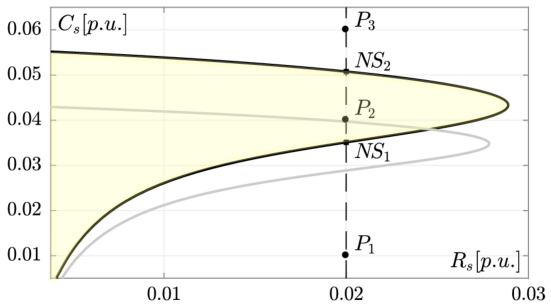

Fig. 2. Bifurcation diagrams on the plane (R_s, C_s) in p.u.

Finally, the NSB does not occur at all if one chooses a value of R_s corresponding to vertical lines that do not intersect the nose-shaped bifurcation curves in Fig. 2. This means that, by properly increasing R_s over a value $R_s^*(L_s)$, the stability of Γ does not depend on C_s.

The following are two relevant conclusions that can be drawn from the bifurcation analysis above: (i) increasing the (equivalent) resistance R_s can prevent instability; and (ii) as L_s decreases, the unstable SSR region shrinks and $R_s^*(L_s)$ decreases.

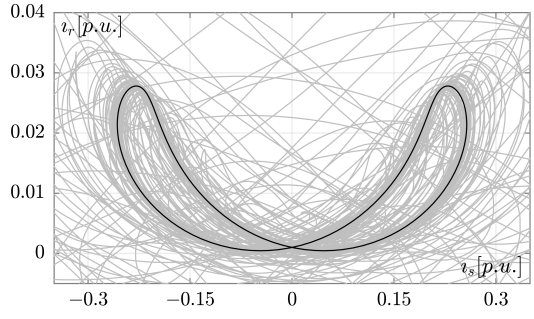

Fig. 3. Trajectories projected on the $(\imath_s, \imath_r)$ plane obtained for the parameters values corresponding to P_2 in Fig. 2.

The discussion above refers to a given set of parameters. It is thus relevant to discuss whether parameter uncertainty can change the behavior of the system. Recent works, e.g., [6]–[8], show that line compensation leads to the IGE with DFIGs configurations. In particular in [7] the authors apply a frequency scanning for various line lengths and always find a resonance (or bifurcation) condition.

According to our several simulation tests, we have also always found that the bifurcation occurs for any given set of machine and transmission line parameters (see for example the grey curve in Fig. 2). These conditions appear to be independent from mechanical equations and the control (in fact, the bifurcation occurs also for squirrel cage induction generators utilized in Type A wind turbines). These facts allow us empirically concluding that the NSB is persistent,[1] at least for parameters in the range of values that are of practical interest. Thus, the effect of parameter uncertainty is to "move" the bifurcation but not to "destroy" it. Moreover, for the well-konwn properties of continuous equations, small parameter variations lead to small variations of the point at which the NSB occurs.

From a practical point of view, the bifurcation diagram shown in Fig. 2 provides the conditions for which the NSB occurs for a given set of parameters but it can actually also be utilized in the other way round, namely, to deduce the "distance" of a given set of parameters to the bifurcation. The stability margin can be thus imposed by assuming a safety distance similarly to the transmission reliability margin (TRM) defined by NERC to calculate the available transfer capability of a transmission system [12]. The TRM is basically a heuristic margin that takes into account uncertainty and aspects of the power system that are not explicitly modeled. For example, considering the case study discussed in this section, for $R_s = 0.02$ pu, the bifurcation diagram of Fig. 2 shows that it is safe to assume that the NSB does not occur for $C_s > 0.06$ or $C_s < 0.02$. This result is still valid if R_s is varied in a small range to simulate typical parameter uncertainty.

[1]For a difinition of "persistence", the interested reader can refer to [11].

REFERENCES

[1] K. R. Padiyar, *Analysis of Subsynchronous Resonance in Power Systems*, 1st ed., ser. The Springer International Series in Engineering and Computer Science. Springer, US, 1999.

[2] K. Kabiri, H. W. Dommel, and S. Henschel, "A simplified system for subsynchronous resonance studies," in *proceedings of the International Conference on Power Systems Transients, Rio de Janeiro, Brazil*, June 2001.

[3] IEEE Subsynchronous Resonance Task Force of the Dynamic System Performance Working Group Power System Engineering Committee, "First benchmark model for computer simulation of subsynchronous resonance," *IEEE Transactions on Power Apparatus and Systems*, vol. 96, no. 5, pp. 1565–1572, Sept. 1977.

[4] L. Fan, A. Feliachi, and K. Schoder, "Selection and design of a TCSC control signal in damping power system inter-area oscillations for multiple operating conditions," *Electric Power Systems Research*, vol. 62, no. 2, pp. 127–137, 2002.

[5] L. A. Kilgore, L. C. Elliott, and E. R. Taylor, "The prediction and control of self-excited oscillations due to series capacitors in power systems," *IEEE Transactions on Power Apparatus and Systems*, vol. PAS-90, no. 3, pp. 1305–1311, May 1971.

[6] A. E. Leon and J. A. Solsona, "Sub-synchronous interaction damping control for DFIG wind turbines," *IEEE Transactions on Power Systems*, vol. 30, no. 1, pp. 419–428, Jan. 2015.

[7] X. Zhu and Z. Pan, "Study on the influencing factors and mechanism of SSR due to DFIG-based wind turbines to a series compensated transmission system," in *2017 IEEE 26th International Symposium on Industrial Electronics (ISIE)*, June 2017, pp. 1029–1034.

[8] M. A. Chowdhury and G. M. Shafiullah, "SSR mitigation of series-compensated DFIG wind farms by a nonlinear damping controller using partial feedback linearization," *IEEE Transactions on Power Systems*, vol. PP, no. 99, pp. 1–1, 2017.

[9] S. N. Vukosavic, *Electrical machines*. New York, NY, USA: Springer, 2013.

[10] Y. A. Kuznetsov, *Elements of Applied Bifurcation Theory*, 3rd ed. New York: Springer-Verlag, 2004.

[11] H. D. Chiang and L. Fekih-Ahmed, "Persistence of saddle-node bifurcations for general nonlinear systems under unmodeled dynamics and applications," in *IEEE International Symposium on Circuits and Systems*, May 1993, pp. 2656–2659 vol.4.

[12] North American Electric Reliability Council Available Transfer Capability Working Group, "Transmission Capability Margins and Their Use in ATC Determination – White Paper," June 1999, available on-line at: www.nerc.com.